JOURNAL OF SPACECRAFT AND ROCKETS
Vol. 35, No. 4, July–August 1998

Magnus Effects on Stability of Wraparound-Finned Missiles

Ömer Tanrıkulu* and Gökmen Mahmutyazıcıoğlu†
Defense Industries Research and Development Institute (TÜBİTAK–SAGE), Mamak 06261, Ankara, Turkey

Wraparound fins are widely used as aerodynamic stabilizers for unguided missiles. Wraparound-finned configurations have more complicated flight dynamics when compared with configurations with planar fins. General linear free flight dynamic stability criteria of unguided missiles with wraparound fins are well known. However, until now simplified criteria that consider a static side moment due to wraparound fins as the only significant out-of-plane effect have been utilized in design. It is shown that the simplified stability criteria are not reliable, and more general stability criteria that take both the classical Magnus side moment and the static side moment due to wraparound fins into account have to be used. Another outcome is that the roll direction is extremely important in terms of stability of wraparound-finned configurations. A linear free flight dynamic stability analysis of the U.S. Air Force research model is performed as a case study by using available aeroballistic range test data.

Nomenclature

a_∞ = freestream speed of sound, m/s
C_D = drag force coefficient
$C_{D_{\alpha^2}}$ = quadratic drag force coefficient
$C_{l_{p\pm}}$ = roll damping moment stability derivative
C_{l_0} = induced roll moment coefficient
C_{l_δ} = roll moment due to fin cant angle stability derivative
$C_{m_q}, C_{m_{\dot\alpha}}$ = in-plane damping moment stability derivatives
$C_{m_r}, C_{m_{\dot\beta}}$ = out-of-plane damping moment stability derivatives
C_{m_0} = in-plane asymmetry moment coefficient
C_{m_α} = static in-plane moment stability derivative
$C_{m_{\alpha p}}$ = in-plane Magnus moment stability derivative
C_{m_β} = static out-of-plane moment stability derivative
$C_{m_{\beta p}}$ = out-of-plane Magnus moment stability derivative
C_{n_0} = out-of-plane asymmetry moment coefficient
C_{Y_0} = out-of-plane asymmetry force coefficient
C_{Z_0} = in-plane asymmetry force coefficient
C_{Z_α} = static in-plane force stability derivative
C_{Z_β} = static out-of-plane force stability derivative
$\tilde{g}_3$ = third component of gravitational acceleration vector, m/s^2
I_a = axial moment of inertia, kg m^2
I_t = transverse moment of inertia, kg m^2
i = unit imaginary number
k_a = nondimensional axial radius of gyration
k_t = nondimensional transverse radius of gyration
M_∞ = freestream Mach number
m = mass, kg
p, q, r = roll, pitch, and yaw rates in body-fixed reference frame, rad/s
S = reference area, $(\pi/4)\lambda^2$, m^2
s = nondimensional arc length

$$\left(\frac{1}{\lambda}\right)\int_{t_o}^{t} V\,\mathrm{d}t$$

V = speed of missile, m/s
x_{CM} = distance of center of mass from missile tip, m
α = angle of attack, rad
β = angle of side slip, rad
δ = fin cant angle, rad
λ = reference length, missile diameter, m
ξ = complex total angle of attack, $\beta + i\alpha$
ρ_∞ = freestream density, kg/m^3
ψ, θ, ϕ = Euler yaw, pitch, and roll angles, rad

Superscripts

$\tilde{}$ = component in aeroballistic reference frame
$'$ = differentiation with respect to s

Received Oct. 6, 1997; revision received March 25, 1998; accepted for publication March 26, 1998.

*Coordinator, Mechanics and Systems Engineering Research Group (MSMG), PK 16. Member AIAA.
†Chief Research Engineer, Mechanics and Systems Engineering Research Group (MSMG), Flight Dynamics Section, PK 16.

Introduction

TUBE launchers have now become almost a standard feature of unguided missile systems due to packaging conveniences. Aerodynamically stabilized tube-launched missiles have hinged tail fins, which are in their folded position when the missile is inside the launcher. Deployment of the tail fins takes place just after launch due to gyroscopic, aerodynamic, and mechanical forces. Tube launching can have some negative implications in terms of missile external configuration design inasmuch as dimensions of tail fins are constrained geometrically. Wraparound fins (WAF) were introduced as an alternative to planar fins (PF) to partly overcome this problem. On the other hand, it was soon discovered that missile configurations with WAF have complicated aerodynamics and flight dynamics due to lack of mirror symmetry. Intense theoretical, numerical, and experimental research on the subject revealed interesting results.[1–26]

1) Missile configurations with WAF have different roll damping stability derivatives $C_{l_{p\pm}}$ depending on the direction of roll.

2) Missile configurations with WAF have a nonzero induced roll moment C_{l_0} at zero total angle of attack. C_{l_0} strongly depends on M_∞, missile geometry, and wake condition. C_{l_0} changes sign at transonic M_∞ in jet-off flight, whereas no such sign change is observed in the case of jet-on flight. C_{l_0} can have significant effect on roll rate history and, hence, stability and dispersion characteristics.

3) There is a 10% increase in the fin drag coefficient of a missile if WAF is used instead of equivalent PF that have the same projected area.

4) Static aerodynamic characteristics C_{z_α} and C_{m_α} obtained with WAF and with equivalent PF that have the same projected area are very similar.

5) Missile configurations with WAF do not have mirror symmetry. Hence, the presence of stability derivatives such as C_{m_β}, $C_{m_{\dot\beta}}$, C_{m_r}, and $C_{m_{\alpha p}}$ in addition to C_{m_α}, $C_{m_{\dot\alpha}}$, C_{m_q}, and $C_{m_{\beta p}}$ is mathematically possible. Wind-tunnel and aeroballistic range testing has shown that C_{m_β} is significant for configurations with WAF.

6) General linear static and dynamic stability criteria for free flight of missiles with WAF were derived. These criteria were simplified by considering C_{m_β} to be the only significant WAF and out-of-plane effect. A variety of case studies showed that dynamic stability and resonance characteristics strongly depend on C_{m_β}. WAF effects on static stability were found to be insignificant. Missile configurations

with WAF were observed to exhibit circular trajectories in the α vs β plane in cases of both stable and unstable flight.

The presence of C_{l_0} and C_{m_β} has caused many problems for flight dynamicists in the external configuration design of unguided missiles with WAF. The physical mechanisms that cause C_{l_0} are not well understood, and magnitudes of moments that are associated with C_{l_0} and C_{m_β} are much smaller than magnitudes of conventional moments. Hence, accurate experimental determination of C_{l_0} and C_{m_β} through wind-tunnel or aeroballistic range testing is difficult. These problems led some researchers to focus on making small modifications to missile geometry to alleviate adverse effects of WAF. Mostly direct modification of WAF by using tabs, bevels, or slots was considered.[8,13,23] It was shown that introduction of a cavity in the missile base without altering WAF surprisingly enhances dynamic stability WAF.[15,16,19,24,26]

The research on base cavity modification could not provide a satisfactory explanation regarding the improvement of dynamic stability, but it had an important outcome. During the aeroballistic range tests of the U.S. Air Force research model with base cavity, Abate and Hathaway[16,19] were able to identify both $C_{m_{\beta_p}}$ and C_{m_β} data in several cases. It is well known that Magnus moment has a destabilizing effect on rolling missile configurations with PF. Rolling WAF configurations also generate a Magnus moment. Interestingly enough, aeroballisticians have considered the side moment due to WAF characterized by C_{m_β} as the only significant out-of-plane effect in linear free flight dynamic stability analysis of such missiles. Omission of Magnus effects can be attributed to the complicated nature of Magnus phenomena and to the difficulties in accurate theoretical, experimental, or numerical determination of $C_{m_{\beta_p}}$ data.[27] In this paper, a stability analysis of the U.S. Air Force research model with base cavity will be performed by using the available aeroballistic range test data. Different stability criteria will be utilized: a newly developed criterion for configurations with WAF that take both $C_{m_{\beta_p}}$ and C_{m_β} into account,[21,22,26] the conventional criteria for configurations with PF that consider $C_{m_{\beta_p}}$ as the only out-of-plane effect, and finally the conventional simplified criteria for configurations with WAF that consider C_{m_β} as the only out-of-plane effect.

Linear Free Flight Dynamic Stability Analysis

The complex transverse equation of motion of a slightly asymmetric unguided missile with WAF in free flight can be expressed as follows in the aeroballistic reference frame[22]:

$$\tilde{\xi}'' + [H + i(I - P)]\tilde{\xi}' - [(M + PU) + i(N + PT)]\tilde{\xi} = G + iAe^{i\phi} \tag{1}$$

In Eq. (1) the independent variable is the nondimensional arc length s. Coefficients of Eq. (1) are defined as

$$H = -\left[C^*_{Z_\alpha} + 2C^*_D + \left(1/2k_t^2\right)\left(C^*_{m_q} + C^*_{m_{\dot\alpha}}\right)\right] \tag{2}$$

$$I = -\left[C^*_{Z_\beta} + \left(1/2k_t^2\right)\left(C^*_{m_r} + C^*_{m_{\dot\beta}}\right)\right] \tag{3}$$

$$P = (I_a/I_t)(\tilde{p}\lambda/V) \tag{4}$$

$$M = \left(1/k_t^2\right)C^*_{m_\alpha} \tag{5}$$

$$N = \left(1/k_t^2\right)C^*_{m_\beta} \tag{6}$$

$$T = \left(1/2k_a^2\right)C^*_{m_{\beta_p}} - C^*_{Z_\alpha} - C^*_D \tag{7}$$

$$U = C^*_{Z_\beta} - \left(1/2k_a^2\right)C^*_{m_{\alpha_p}} \tag{8}$$

$$G \approx (\lambda/V^2)\tilde{\mathbf{g}}_3 P \tag{9}$$

$$A = \left(1/k_t^2\right)\left(C^*_{m_0} + iC^*_{n_0}\right) + P[(I_t/I_a) - 1]\left(C^*_{Y_0} + iC^*_{Z_0}\right) \tag{10}$$

$$k_{a,t} = \sqrt{I_{a,t}/m\lambda^2} \tag{11}$$

$$C^* = (\rho_\infty S\lambda/2m)C \tag{12}$$

Equation (1) can be considered as a linear differential equation with constant coefficients when M_∞ and p are slowly changing functions of time. Hence, the solution of Eq. (1) can be expressed as

$$\tilde{\xi} = \tilde{\xi}_g + K_1 e^{i\phi_1} + K_2 e^{i\phi_2} + K_3 e^{i\phi_3} \tag{13}$$

where

$$\tilde{\xi}_g = -\frac{G}{(M + PU) + i(N + PT)} \tag{14}$$

$$K_j = K_{j_0} e^{\lambda_j s} \qquad (j = 1, 2) \tag{15}$$

$$\phi_j = \phi_{j_0} + \phi'_j s \qquad (j = 1, 2) \tag{16}$$

$$\lambda_j + i\phi'_j = \tfrac{1}{2}\left\{-H + i(P - I) \mp \sqrt{4(M + PU) + H^2 - (I - P)^2 + i[2H(I - P) + 4(N + PT)]}\right\} \qquad (j = 1, 2) \tag{17}$$

$$\phi_3 = \phi_{3_0} + \phi \tag{18}$$

In Eq. (13), $K_j e^{i\phi_j}$ $(j = 1, 2)$ terms represent the homogeneous solution, whereas $\tilde{\xi}_g$ and $K_3 e^{i\phi_3}$ are the particular solutions due to gravity and configurational asymmetry, respectively. The stability of an unguided missile with WAF in free flight can be examined by using Eq. (17). After a few derivations one can obtain the following expression for the modal damping factors λ_j $(j = 1, 2)$:

$$\lambda_j = -\frac{1}{2}\left[H \mp \frac{2(N + PT) - H(P - I)}{\sqrt{(P - I)^2 - 4(M + PU)}}\right] \tag{19}$$

Dynamic stability of the missile is ensured if both of the modal damping factors λ_j $(j = 1, 2)$ have negative values during all phases of flight:

$$\lambda_j \le 0 \qquad (j = 1, 2) \tag{20}$$

Inequality (20) can be expanded as follows:

$$H \ge 0 \tag{21}$$

$$|H| \ge \left|\frac{2(N + PT) - H(P - I)}{\sqrt{(P - I)^2 - 4(M + PU)}}\right| \tag{22}$$

If inequality (22) is further expanded, one can obtain a quadratic stability condition in terms of the gyroscopic roll rate P:

$$T(T - H)P^2 + (UH^2 + 2TN - HN + THI)P + (MH^2 + N^2 + NHI) \le 0 \tag{23}$$

$$\left(P - P_{\text{dyn}_1}\right)\left(P - P_{\text{dyn}_2}\right) \le 0 \tag{24}$$

Constraints (21) and (24) indicate that an unguided missile with WAF in free flight is dynamically stable if it has positive in-plane damping and its roll rate stays in an interval that is specified by P_{dyn_1} and P_{dyn_2}. Actual roll rotational rates corresponding to P_{dyn_1} and P_{dyn_2} can be determined as

$$p_{\text{dyn}_j} = (I_t/I_a)(V/\lambda)P_{\text{dyn}_j} \qquad (j = 1, 2) \tag{25}$$

In the case of a missile with PF that has both rotational and mirror symmetry, I, N, and $U = 0$. Hence, Eq. (23) becomes

$$T(T - H)P^2 + MH^2 \le 0 \tag{26}$$

Constraint (26) is a quadratic inequality as well, but $P_{\text{dyn}_1} = -P_{\text{dyn}_2}$ in contrast to the earlier, more general case. In the case of a stability analysis of a missile with WAF in which C_{m_β} is considered as

Table 1 Reference and inertial data of a typical test model[16,19]

D, m	S, m^2	a_∞, m/s	ρ_∞, kg/m^3	m, kg	I_a, kg · m^2	I_t, kg · m^2	x_{CM}, m
1.91×10^{-2}	2.85×10^{-4}	344	1.2	0.143	7.2×10^{-6}	4.8×10^{-4}	0.099

Table 2 Aerodynamic data of tests 14, 25, 20, and 26 (Refs. 16 and 19)

Test no.	M_∞	C_D	$C_{D_{\alpha^2}}$	C_{Z_α}	C_{m_α}	C_{m_β}	C_{m_q}	$C_{m_{\beta p}}$	C_{l_p}	$C_{l_\delta}\delta$
14	1.002	0.841	3.000	−10.50	−39.766	1.33	−477.8	−138.89	−6.616	0.156
25	1.658	0.865	2.500	−8.44	−13.886	−0.35	−394.5	−27.45	−2.371	0.135
20	1.723	0.845	2.500	−8.22	−12.243	−0.59	−364.0	−20.00	−9.858	−0.260
26	1.861	0.842	2.500	−7.01	−8.882	−0.99	−326.4	57.01	−2.695	0.025

the only significant WAF and out-of-plane effect, inequality (23) is reduced to

$$-HNP + MH^2 + N^2 \leq 0 \tag{27}$$

Constraint (27) is a linear inequality in terms of P that specifies lower and upper limits of roll rate p for dynamic stability when $p > 0$ and $p < 0$, respectively.

The classical yaw–pitch–roll resonance rate of a statically stable missile with WAF can be approximated to be the same as that of a missile with equivalent PF:

$$p_{\text{res}} \approx (V/\lambda)\sqrt{-M} \tag{28}$$

Case Study

As was mentioned earlier, Abate and Hathaway[16,19] carried out aeroballistic range tests of the U.S. Air Force research model with base cavity. They compared their results with the ones that were obtained from previous tests of the same model without base cavity. The basic geometry of the model with base cavity is presented in Fig. 1 (details can be found in Ref. 16). Reference and inertial data of a typical model are given in Table 1. Abate and Hathaway tested 15 models with base cavity, at different Mach numbers; 13 of them had a fin cant angle of −2 or +2 deg, whereas 2 models had no fin cant. High roll rates were observed in the tests of models with canted fins. Hence, in four of these tests, analysis of motion data resulted in identification of both C_{m_β} and $C_{m_{\beta p}}$ stability derivatives at the same time. Aerodynamic data that were obtained from these tests are presented in Tables 2 and 3. No nonlinear coefficients were identified other than $C_{D_{\alpha^2}}$. In Table 4 the probable errors of the curve fitting are presented. The quality of the curve fit for roll angle is poor for all four cases. On the other hand, numerically predicted and experimentally measured motion data are in good agreement with each other.[16,19] Nondimensional axial and transverse radii of gyration are $k_a = 0.372$ and $k_t = 3.041$, respectively, whereas $\rho_\infty S\lambda/2m$ has a value of 2.278×10^{-5}. The coefficients of the transverse equation of motion (1) for the four cases are presented in Table 5. $H \geq 0$ for all four tests; hence, transverse damping constraint (21) is satisfied. In Table 6 the gyroscopic roll rate limits for dynamic stability are presented for the four tests, which were calculated by using the data of Table 5. The roll rate limit denoted by C (C_{m_β} only) is both qualitatively and quantitatively different from the limits denoted by A (C_{m_β} and $C_{m_{\beta p}}$) and B ($C_{m_{\beta p}}$ only). The difference between roll rate limits A and B is quantitative. C_{m_β} introduces asymmetry into $P_{\text{dyn}_{1,2}}$ values, which are shifted up or down, both at the same time. In Table 7, yaw–pitch–roll resonance roll rate values of the four cases that were calculated using Eq. (28) are presented. Figures 2–5 and 6–9 show p vs t and ψ vs θ graphs, respectively, for tests 14, 25, 20, and 26 as obtained from six-degree-of-freedom numerical simulations (fourth-order Runge–Kutta, fixed time-step size) with reference, inertial, and aerodynamic data of Tables 1–3.

Discussion

In Figs. 2–5 dynamic stability roll rate limits denoted by A (C_{m_β} and $C_{m_{\beta p}}$) and B ($C_{m_{\beta p}}$ only) corresponding to Table 6 are plotted in addition to the time variation of roll rate p. The stability roll rate limit denoted by C (C_{m_β} only) is not shown in the Figs. 2–5 because its magnitude is much larger than other data for all

Table 3 Configurational asymmetry data of tests 14, 25, 20, and 26 (Refs. 16 and 19)

Test no.	M_∞	C_{Z_0}	C_{Y_0}	C_{m_0}	C_{n_0}
14	1.002	0.038	0.443	−0.466	−0.172
25	1.658	0.000	0.000	0.000	0.000
20	1.723	0.000	0.000	0.485	−0.032
26	1.861	0.000	0.000	−0.017	0.040

Table 4 Probable errors of curve fitting for tests 14, 25, 20, and 26 (Refs. 16 and 19)

Test no.	x, m	$y - z$, m	$\theta - \psi$, deg	ϕ, deg
14	0.0028	0.0009	0.205	19.840
25	0.0013	0.0011	0.242	48.460
20	0.0006	0.0009	1.158	9.514
26	0.0012	0.0006	0.120	9.444

Table 5 Coefficients of transverse equation of motion for tests 14, 25, 20, and 26

Test no.	M_∞	$M \times 10^{-5}$	$N \times 10^{-6}$	$H \times 10^{-4}$	$T \times 10^{-3}$
14	1.002	−9.795	3.276	7.893	11.183
25	1.658	−3.420	−0.862	6.387	−2.081
20	1.723	−3.016	−1.453	5.970	−1.474
26	1.861	−2.188	−2.438	5.233	4.821

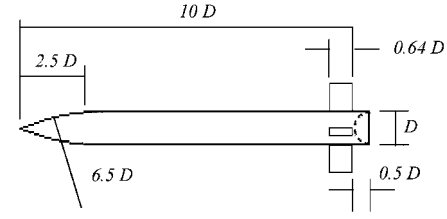

Fig. 1 Test model with WAF and base cavity.[16,19]

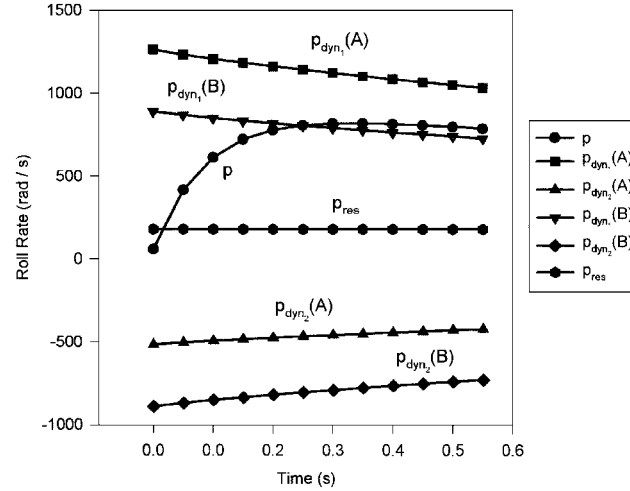

Fig. 2 Time variation of roll rate for test 14.

Table 6 Dynamic stability gyroscopic roll rate limits for the tests 14, 25, 20, and 26

Test no.	A: $P_{\text{dyn}_1} \times 10^{-3}$	A: $P_{\text{dyn}_2} \times 10^{-3}$	B: $P_{\text{dyn}_1} \times 10^{-3}$	B: $P_{\text{dyn}_2} \times 10^{-3}$	C: $P_{\text{dyn}} \times 10^{-2}$
14	0.958	−0.392	0.675	−0.675	−1.945
25	1.205	−1.936	1.570	−1.570	2.399
20	1.038	−2.726	1.876	−1.876	0.996
26	1.075	−0.002	0.538	−0.538	0.004

Table 7 Yaw–pitch–roll resonance roll rates for tests 14, 25, 20, and 26, rad/s

Test no.:	14	25	20	26
p_{res}	179.1	175.1	170.9	157.2

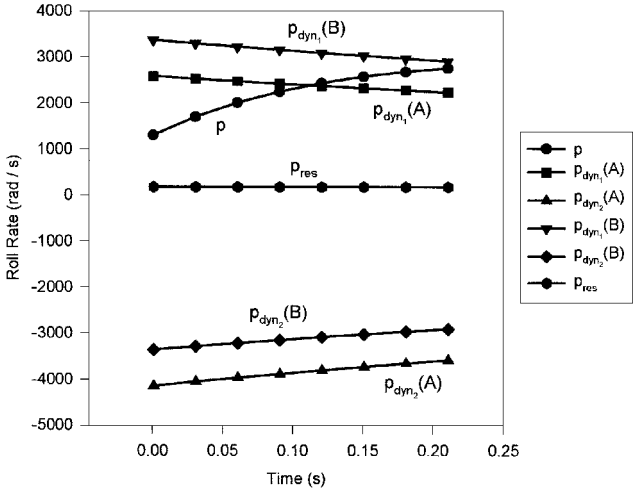

Fig. 3 Time variation of roll rate for test 25.

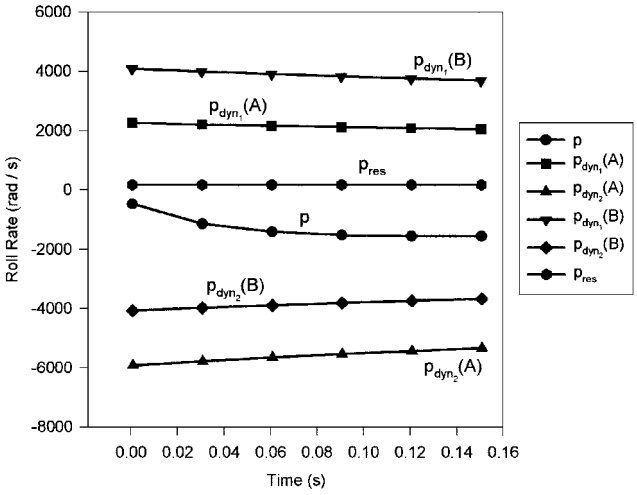

Fig. 4 Time variation of roll rate for test 20.

tests. One can obtain completely wrong results in stability analysis of rolling WAF configurations when both C_{m_β} and $C_{m_{\beta p}}$ are present and the type C criterion is used.

As was stated earlier, if one considers $C_{m_{\beta p}}$ to be the only out-of-plane moment, then $p_{\text{dyn}_1} = -p_{\text{dyn}_2}$. Introduction of C_{m_β} destroys this symmetry. In the case of tests 14 and 26, C_{m_β} shifts both p_{dyn_1} and p_{dyn_2} data upward (Figs. 2 and 5). The shift is especially significant in the case of test 26. In the case of tests 25 and 20, C_{m_β} shifts both p_{dyn_1} and p_{dyn_2} data downward (Figs. 3 and 4).

In the case of test 14, criterion B predicts unstable flight because p crosses the p_{dyn_1} limit. Stability criterion A and Fig. 6 indicate that flight is stable in test 14. In this case, C_{m_β} enhances dynamic stability by shifting the roll rate limit p_{dyn_1} upward. One must note that C_{m_β} would have caused instability if the model was rolled in a negative direction because p_{dyn_2} is shifted upward as well. Similar analysis can be made for the other three tests by examining Figs. 3–5 and 7–9.

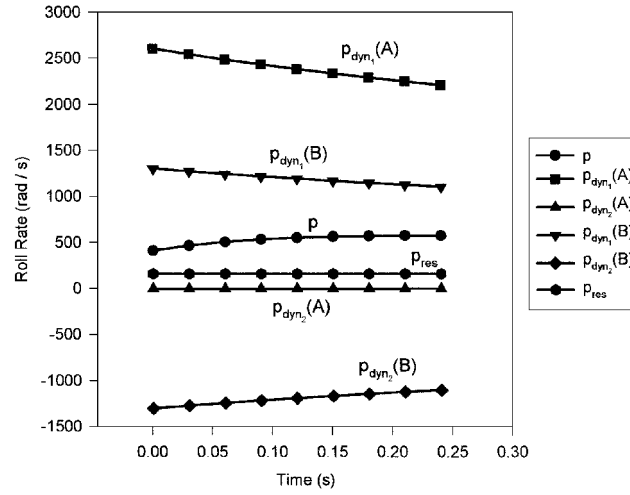

Fig. 5 Time variation of roll rate for test 26.

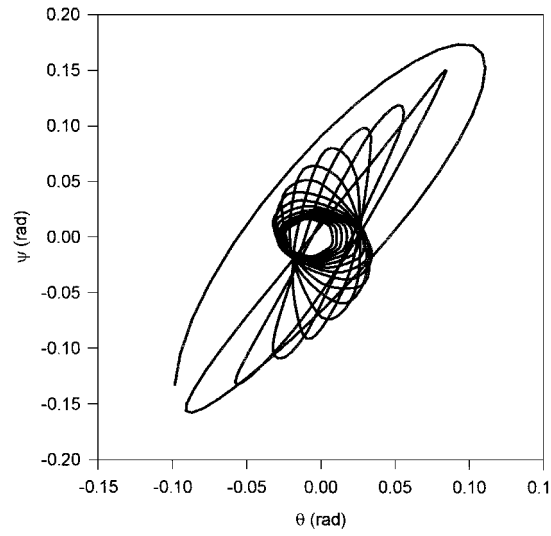

Fig. 6 Graph for test 14, ψ vs θ.

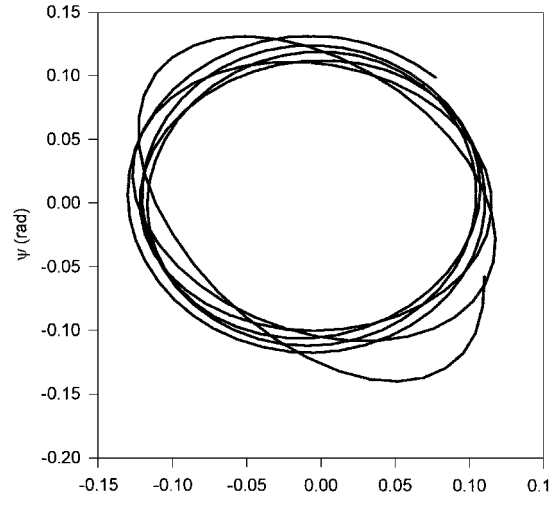

Fig. 7 Graph for test 25, ψ vs θ.

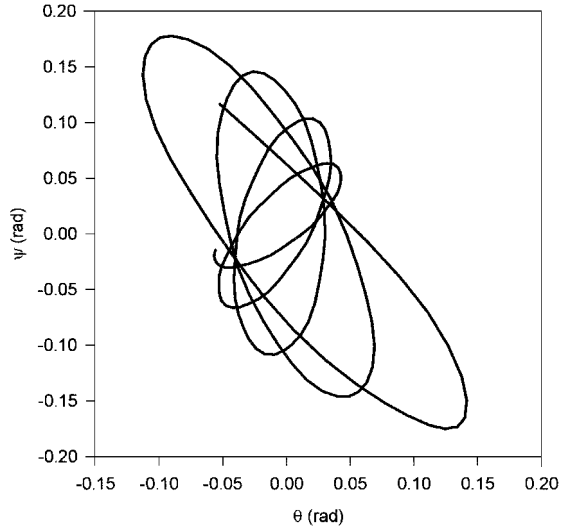

Fig. 8 Graph for test 20, ψ vs θ.

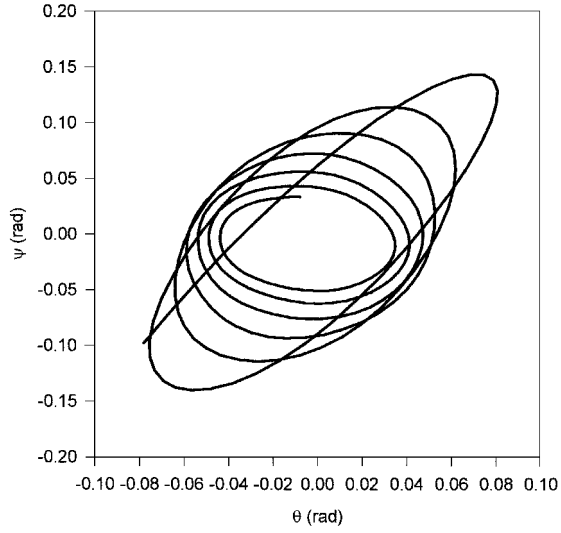

Fig. 9 Graph for test 26, ψ vs θ.

Conclusion and Recommendations

Linear free flight dynamic stability analysis of the U.S. Air Force research model with WAF was performed by using the available aeroballistic range test data. Roll rate limits for dynamic stability were determined by using three different criteria, and the results were compared qualitatively and quantitatively. This was followed by an assessment of accuracy through a comparison of stability predictions of different criteria with the behavior observed in numerically generated six-degrees-of-freedom motion data. Conclusions are summarized as follows.

1) Accurate linear free flight dynamic stability analysis of an unguided missile with WAF can only be performed by using criterion A (C_{m_β} and $C_{m_{\beta p}}$). Stability analyses with criterion B ($C_{m_{\beta p}}$ only) and, especially, with criterion C (C_{m_β} only) give wrong results. This is an extremely important result because until now aeroballisticians have used criterion C only in their dynamic stability analyses.

2) Lack of mirror symmetry of WAF configurations is well reflected by criterion A (shift of p_{dyn_1} and p_{dyn_2} data upward or downward).

3) Roll direction is extremely important in terms of the dynamic stability of WAF unguided missiles. Designing stable WAF configurations with rotational symmetry only is much more difficult than designing PF configurations with mirror and rotational symmetry because the direction of the shift of p_{dyn} curves is different for different Mach numbers. Hence, positive or negative roll rate may be preferable for different phases of flight at different Mach numbers. Roll programming with bevels or tabs is important not only in dealing with effects of induced roll moment C_{l_0} but also in maintaining $p_{\text{dyn}_1} < p < p_{\text{dyn}_2}$.

Recommendations are summarized as follows.

1) As was mentioned in the Introduction, WAF configurations have roll direction-dependent roll damping stability derivatives $C_{l_{p\pm}}$. They can also be expected to have roll direction-dependent Magnus moment stability derivatives $C_{m_{\beta p\pm}}$. Two tests of Abate and Hathaway that were performed at the same Mach number but with opposite roll directions indicated such a phenomenon. They were not discussed herein because it was concluded that more tests are necessary.

2) As was also mentioned in the Introduction, WAF configurations may generate moments that are characterized by $C_{m_{\dot\beta}}$, C_{m_r}, and $C_{m_{\alpha p}}$. Further research is needed in this area.

3) Surprisingly, no research has been carried out on nonlinear aeroballistics (analysis or identification) of WAF configurations. Further research is needed in this area.

Acknowledgments

This paper was prepared as a part of the T-104 support project of the NATO AGARD Flight Vehicle Integration Panel. The project was jointly run by TÜBİTAK-SAGE and the U.S. Air Force Wright Laboratory, Eglin Air Force Base. The authors wish to express their appreciation to G. L. Abate and G. L. Winchenbach of the U.S. Air Force Wright Laboratory for supplying information about tests with base cavity and for their critical comments on the subject.

References

[1]Dahlke, C. W., and Craft, J. C., "The Effect of Wrap-Around Fins on Aerodynamic Stability and Rolling Moment Variations," U.S. Army Missile Research Development and Engineering Lab., RD-73-17, Redstone Arsenal, AL, July 1973.

[2]Stevens, F. L., "Analysis of the Linear Pitching and Yawing Motion of Curved Finned Missiles," U.S. Naval Weapons Lab., NWL TR-2989, Dahlgren, VA, Oct. 1973.

[3]Stevens, F. L., On, T. J., and Clare, T. A., "Wrap-Around vs Cruciform Fins: Effects on Rocket Flight Performance," AIAA Paper 74-777, Aug. 1974.

[4]Daniels, P., and Hardy, S. R., "Roll Rate Stabilization of a Missile Configuration with Wrap-Around Fins," *Journal of Spacecraft and Rockets*, Vol. 13, No. 7, 1975, pp. 446–448.

[5]Humphrey, A. J., and Dahlke, C. W., "A Summary of Aerodynamic Characteristics for Wrap-Around Fins from Mach 0.3 to 3.0," U.S. Army Missile Research Development Command, TD-77-5, Redstone Arsenal, AL, March 1977.

[6]Hardy, S. R., "Non-Linear Analysis of the Rolling Motion of a Wrap-Around Fin Missile at Angles of Attack from 0° to 90° in Compressible Flow," U.S. Naval Surface Weapons Center, NSWC/DL-TR-3727, Dahlgren, VA, Sept. 1977.

[7]Catani, U., Bertin, J., De Amicis, R., Masullo, S., and Bouslog, S., "Aerodynamic Characteristics for a Slender Missile with Wrap-Around Fins," *Journal of Spacecraft and Rockets*, Vol. 20, No. 2, 1982, pp. 122–128.

[8]Dahlke, C. W., Deep, R. A., and Oskay, V., "Techniques for Roll Tailoring for Missiles with Wrap-Around Fins," AIAA Paper 83-0463, Jan. 1983.

[9]Bar Haim, B., and Seginer, A., "Aerodynamics of Wrap-Around Fins," *Journal of Spacecraft and Rockets*, Vol. 20, No. 4, 1983, pp. 339–345.

[10]Whyte, R. H., Hathaway, W. H., Buff, R. S., and Winchenbach, G. L., "Subsonic and Transonic Aerodynamics of a Wrap-Around Fin Configuration," AIAA Paper 85-0106, Jan. 1985.

[11]Kim Hoon, Y., and Winchenbach, G. L., "Roll Motion of a Wrap-Around Fin Configuration at Subsonic and Transonic Mach Numbers," *Journal of Guidance, Control, and Dynamics*, Vol. 9, No. 2, 1986, pp. 253–255.

[12]Winchenbach, G. L., Buff, R. S., Whyte, R. H., and Hathaway, W. H., "Subsonic and Transonic Aerodynamics of a Wrap-Around Fin Configuration," *Journal of Guidance, Control, and Dynamics*, Vol. 9, No. 6, 1986, pp. 627–632.

[13]Abate, G. L., and Winchenbach, G. L., "Aerodynamics of Missiles with Slotted Fin Configurations," AIAA Paper 91-0676, Jan. 1991.

[14]Vitale, R. E., Abate, G. L., Winchenbach, G. L., and Riner, W., "Aerodynamic Test and Analysis of a Missile Configuration with Curved Fins," *Proceedings of the AIAA Atmospheric Flight Mechanics Conference*, AIAA, Washington, DC, 1992, pp. 788–797 (AIAA Paper 92-4495).

[15]Sjöquist, A., "Wrap-Around Fins—Neat and Not So Nasty," *13th International Symposium on Ballistics* (Stockholm, Sweden), National Defense Research Establishment, Stockholm, Sweden, 1992, pp. 107–114.

[16]Abate, G. L., and Hathaway, W., "Aerodynamic Test Results: WAF—Base Cavity Model," Aeroballistic Research Facility, F08635-90-C-0038,

Air Force Armament Directorate, U.S. Air Force Wright Lab., Eglin AFB, FL, May 1993.

[17]Abate, G. L., and Cook, T., "Analysis of Missile Configurations with Wrap-Around Fins Using Computational Fluid Mechanics," AIAA Paper 93-3631, Aug. 1993.

[18]Swenson, M. W., Abate, G. L., and Whyte, R. H., "Aerodynamic Test and Analysis of Wrap-Around Fins at Supersonic Mach Numbers Utilizing Design of Experiments," AIAA Paper 94-0200, Jan. 1994.

[19]Abate, G., and Hathaway, W., "Aerodynamic Test and Analysis of Wrap-Around Fins with Base Cavities," AIAA Paper 94-0051, Jan. 1994.

[20]Edge, H. L., "Computation of the Roll Moment for a Projectile with Wrap-Around Fins," *Journal of Spacecraft and Rockets*, Vol. 31, No. 4, 1994, pp. 615–620.

[21]Önen, C., Tanrıkulu, Ö., and Mahmutyazıcıoğlu, G., "Flight Mechanics of Unguided Missiles with Wrap-Around Fins," TÜBİTAK-SAGE, Rept. 93/4-7, SI 94/31, 22192, Ankara, Turkey, Nov. 1994.

[22]Tanrıkulu, Ö., Önen, C., Mahmutyazıcıoğlu, G., and Bektaş, İ., "Linear Stability Analysis of Unguided Missiles with Wrap-Around Tail Fins in Free Flight," AGARD Flight Vehicle Integration Panel Specialist Meeting on Subsystem Integration for Tactical Missiles, Paper 5, Oct. 1995.

[23]Abate, G. L., and Winchenbach, G. L., "Analysis of Wrap-Around Fin and Alternate Deployable Fin Systems for Missiles," AGARD Flight Vehicle Integration Panel Specialist Meeting on Subsystem Integration for Tactical Missiles, Paper 4, Oct. 1995.

[24]Struck, J. A., "Effects of Base Cavity Depth on a Free Spinning Wrap-Around Fin Missile Configuration," M.S. Thesis, Aeronautical Engineering Dept., U.S. Air Force Inst. of Technology, Wright–Patterson AFB, OH, Dec. 1995.

[25]Tilmann, C. P., Huffmann, R. E., Jr., Buter, T. A., and Bowersox, R. D. W., "Characterization of the Flow Structure in the Vicinity of a Wrap-Around Fin at Supersonic Speeds," AIAA Paper 96-0190, Jan. 1996.

[26]Tanrıkulu, Ö., and Mahmutyazıcıoğlu, G., "Wrap-Around Finned Missiles: Neat but Nasty," AIAA Paper 97-3493, Aug. 1997.

[27]Platou, A. S., "Magnus Characteristics of Finned and Non-Finned Missiles," *AIAA Journal*, Vol. 3, No. 1, 1965, pp. 83–90.

R. M. Cummings
Associate Editor